IET Generation, Transmission & Distribution

Research Article

Hybrid cuckoo search algorithm and grey wolf optimiser-based optimal control strategy for performance enhancement of HVDC-based offshore wind farms

ISSN 1751-8687
Received on 25th May 2019
Revised 30th November 2019
Accepted on 3rd February 2020
E-First on 25th March 2020
doi: 10.1049/iet-gtd.2019.0801
www.ietdl.org

Hassan Y. Mahmoud[1] ✉, Hany M. Hasanien[2], Ahmed H. Besheer[3], Almoataz Y. Abdelaziz[4]

[1]Electrical Engineering Division in Engineering for the Petroleum and Process Industries (Enppi), 1 (A) Ahmed El-Zomor Street, 8th District, Nasr City, Cairo, Egypt
[2]Electrical Power and Machines Department, Faculty of Engineering, Ain Shams University, Cairo 11517, Egypt
[3]Environmental Studies and Research Institute University of Sadat City, Sadat City 32897, Egypt
[4]Faculty of Engineering and Technology, Future University in Egypt, Cairo, Egypt
✉ *E-mail: hassanyousef@enppi.com*

Abstract: The hybridisation of two or more algorithms is recently emerging to detect superior solutions to the optimization troubles. In this study, a new hybrid cuckoo search algorithm and grey wolf optimiser (CSA–GWO) optimisation technique is exercised and exhibited to optimally design and tune the controller parameters installed in the voltage source converter (VSC) of an offshore wind farm (OWF). One of the widely used control strategies for VSC is the proportional–integral (PI) closed-loop control system. The new hybrid optimisation algorithm is used to design and tune the PI controllers' parameters to improve the performance of OWF. It shall be mentioned that these parameters are usually hard to obtain owing to the high level of embedded non-linearity in such energy systems. The performance of such optimally designed PI controllers is presented in both dynamic and transient conditions. To examine the realistic stability of the proposed algorithm, real wind speed pattern has been captured from Egypt wind farm at Zafarrana and simulated. The obtained results from this new hybrid optimisation CSA -GWO control system reflect its superiority over other traditional algorithms, such as genetic algorithm, especially during symmetrical and unsymmetrical faults. CSA–GWO algorithm was examined using MATLAB/Simulink.

1 Introduction

Effective renewable energies such as wind, solar, and hydro energy have drawn global attention and concentration during the last period of time, as a result of their ability to reduce the harmful environmental impact namely, gaseous emissions and controlling the planet heating [1–3]. Among those renewable energy resources, wind energy has become one of the most leading trends in power production worldwide due to its economic viability [4]. Wind energy generally can be reaped either onshore or offshore based on the chosen location of the wind farm, where the onshore wind stations are used heavily [5]. In the last few years, OWFs have attractive increasing interest owing to the greater unused energy sources together with better wind circumstances [5, 6]. For the time being, the capacities of the offshore wind farm (OWF) and its distance from the shore are increased at an unprecedented rate [3].

Permanent magnet synchronous generator (PMSG) is considered the most popular generator unit connecting with variable speed wind turbine (VSWT). In PMSG, a gear box is not required and the generator's stator connection with the grid is conducted through a fully rated converter [7, 8]. Although, this kind of generator is characterised by the expensive materials of permanent magnet and its large outer diameter, which offers a number of advantages that make it a good choice for VSWT applications such as low weighing and compact size [9, 10]. Over and above, PMSG type is more efficient, less maintenance, more reliable, and no extra supply for magnetic field excitation [4, 6, 11]. Also, lastly, PMSG can facilely offer maximum power point tracking (MPPT) capabilities [12].

Classical proportional–integral (PI) controllers are used in many applications owing to their robust, strength, and stabilisation [13, 14]. In general, a cascaded control scheme is considered as one of the main common controller techniques that can be used in the converter systems [13, 14]. It consists of four PI controllers, where two are located in the inner loop while the other two are in the outer loop. This control structure is very complicated and consumes for a long time. It is even worse if multiple cascaded controllers are used in the same system.

Consequently, many methods have been used to fine tune the PI controllers' parameters such Ziegler–Nichols method [13–16], symbiotic organisms search [17, 18], many artificial intelligence methods (such as artificial neural network [19], parallel fuzzy controller [20], Takagi–Sugeno fuzzy system [21], and neuro-fuzzy system [22, 23]) and adaptive searching mechanism or evolutionary computation algorithms (genetic algorithm (GA) [24–27], particle swarm optimisation [28–30], and grey wolf optimisation [31–34]). An evolutionary algorithm is representing a randomised search process that is inspired by natural behaviour and the social manner of species. Many researchers have suggested a computational framework and arrangement look for solutions in order to emulate the species' behaviour that is consisted of learning, adaption, and evolution.

The essential goal of this study is to propose an algorithm using the new approach, hybrid cuckoo search algorithm and grey wolf optimiser (CSA–GWO) algorithm, to find the optimal PI controllers' parameters used in VSWT-based PMSG system (mainly two voltage source converter (VSC), each has three cascaded PI controller parameters with six design variables) and also in VSC-based high-voltage direct current (HVDC)-transmission system (mainly two VSCs, each has four cascaded PI controller parameters with eight design variables).

The efficiency and validation of the design parameters using the new hybrid algorithm are thereafter compared with that acquired from the GA technique under the symmetrical and unsymmetrical fault conditions at the grid side. GA technique is one of the evolutionary-based techniques, and it has been utilised in a lot of applications but GA suffers from some major difficulties such as long processing time and confusion in a local minimum. Consequently, the new hybrid algorithm has been suggested to overcome the above-mentioned demerits and weakness.

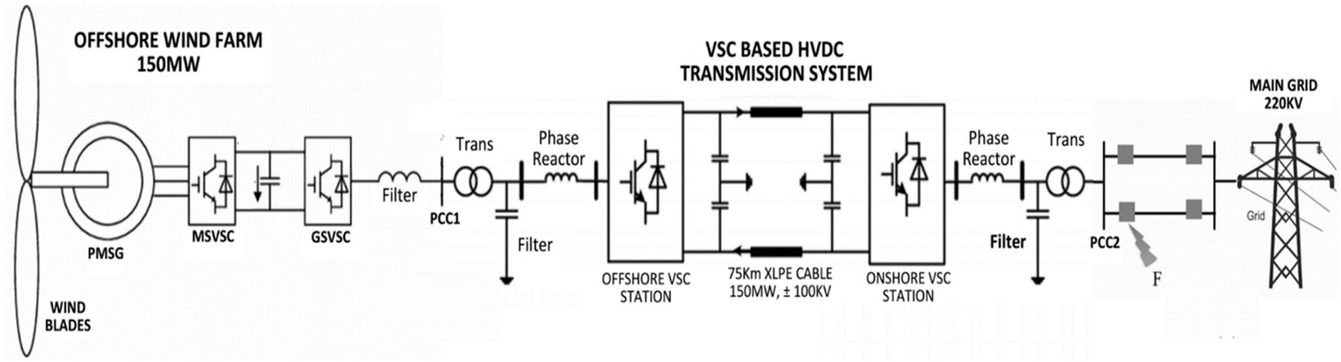

Fig. 1 *Overall single line diagram of OWF with VSC–HVDC system*

Table 1 PMSG parameters

PMSG	Rating
rated power, MW	150
rated voltage, V	690
frequency, Hz	20
number of poles	150
stator resistance, p.u.	0.01
*d*_axis reactance, p.u.	1.0
*q*_axis reactance, p.u.	0.7
flux linkage, p.u.	1.4
inertial, p.u.	0.5

The simulation analysis related to OWF is executed in MATLAB/Simulink simulation environment. The effectiveness of the design model using the new hybrid algorithm is widely confirmed by the simulation records. Finally, it is concluded that the suggested optimal designed process in this study is more efficient to define the controllers' parameters of VSC and to fulfil the fault ride through (FRT) capability of the wind farm during network disturbances than other techniques.

This paper is ordered as follows. The mathematical model of the wind system is demonstrated in Section 2. The mathematical model of the offshore variable speed wind farm-based PMSG is outlined in Section 3, while the same is demonstrated in Section 4 but for VSC-based HVDC. In Section 5, the proposed optimal design is presented with its detailed optimisation procedures. Section 6 shows the simulation results. Finally, the paper is concluded in Section 7.

2 Overall system modelling

The studied system in this study consists of an OWF, three-level VSC–HVDC terminal stations, HVDC cables, and infinite bus of the grid as shown in Fig. 1. The OWF includes VSWT driving a PMSG that is connected with the main grid through two (offshore/onshore) VSC stations. To accelerate the simulation process, the overall OWF model is considered and the rated power capacity of the wind farm is 150 MW, where some of the wind generators of small size are replaced by one large generator [7]. The PMSG parameters are presented in Table 1 [7]. The offered system configuration is connected to the main electrical network via a transmission system. Consequently, the generated active power from OWF has been transmitted into the main network using HVDC cables. The available HVDC cable model in MATLAB/Simulink software library is utilised in the proposed simulation. Each component/element included in the studied model is demonstrated below.

3 Offshore wind generation system

3.1 Wind system principle and configuration

The basic components of the wind system commonly composed of a turbine connected to a generator set. The dynamic behaviour concerning the wind system configuration is explained in [4], where the dynamic mathematical model of the wind turbine is expressed as follows:

$$P_{\mathrm{m}} = 0.5\rho S C_{\mathrm{p}}(\lambda, \beta) V_{\mathrm{w}}^{3} \tag{1}$$

where P_{m} is the extracted mechanical power, V_{w} is wind speed (m/s), S is the circular swept area $(S = \pi R^2)$, R is the turbine blade radius, ρ is the air density (kg/m^3), C_{p} is used to specify the portion of the available power included in the wind system that is converted into a mechanical power with maximum value of 0.593. C_{p} is dependent on the tip speed ratio (λ) and blade pitch angle (β) as represented in (2) and (3) [35]

$$C_{\mathrm{p}}(\lambda, \beta) = 0.5\left(\frac{116}{\lambda_{\mathrm{i}}} - 0.4\beta - 5\right)\mathrm{e}^{-21/\lambda_i} \tag{2}$$

$$\lambda_i = \frac{1}{\left((1/\lambda + 0.08\beta)\ - \left(0.035/\ 1 + \beta^3\right)\right)} \tag{3}$$

3.2 MPPT algorithm

The operating point of the turbine should be maintained at the optimal value (λ_{op}) to extract the maximum available power from the wind system at a given speed [36–38].

The optimal torque control algorithm is one of the MPPT methods and it is used to adapt the rotor speed based on the optimal torque at various wind speeds. The rotor rotational speed (Ω_{ref} in rad/s) is used to represent the optimum extracted mechanical power from the wind as follows:

$$P_{\mathrm{m,op}} = K_{\mathrm{op}}\, \Omega_{\mathrm{ref}}^{3} \tag{4}$$

where

$$K_{\mathrm{op}} = \frac{0.5\rho\pi\, C_{\mathrm{p,op}} R^5}{\lambda_{\mathrm{op}}^{3}} \tag{5}$$

$$\Omega_{\mathrm{ref}} = \lambda_{\mathrm{op}}\frac{V_{\mathrm{w}}}{R} \tag{6}$$

3.3 Control strategy for VSCs connected with VSWT–PMSG

The studied control problem is split into two parts, the first one is related to OWF with targets of active and reactive power control and DC voltage regulation. Whereas, the second one is related to the HVDC system from both sides with targets of DC link voltage regulation and constant AC voltage maintaining at point of common coupling (PCC) as illustrated in Section 4.2.

3.3.1 Control strategy for machine side VSC connected to PMSG: A cascaded control technique is used in a power conversion system, i.e. controlling the real and reactive power flow in both directions in the four quadrants of operation. PMSG is connected with a DC transmission system via two back to back

Table 2 HV cable and converter parameters

HV cable	Rating
conductor_radius, m	0.0178
insulator_radius, m	0.0370
copper resistivity, Ω m	1.724×10^{-8}
permittivity	2.3
resistance at 20°C, Ω/km	0.0172
snubber resistance, Ω	5000
snubber capacitance, F	1.0×10^{-6}
internal resistance (Ω)	1.0×10^{-3}

VSCs. The installed VSC at the PMSG side is mainly used to control the extracted P and Q.

The *dq*-axis components of the stator voltage are obtained as presented in (7) and (8), where to achieve the independency of the current control, terms of compensation are inserted to the PI controller output

$$V_{sq} = \Omega\,\varphi_s - L_s\,\Omega\,I_{sd} - \left(R_s I_{sq} + L_s \frac{dI_{sq}}{dt}\right) \tag{7}$$

$$V_{sd} = -L_s\,\Omega\,I_{sq} - \left(R_s I_{sd} + L_s \frac{dI_{sd}}{dt}\right) \tag{8}$$

with

$$R_s I_{sq} + L_s \frac{dI_{sq}}{dt} = k_{p1}\left(i_{q\text{ref}} - i_q\right) + k_{i1}\int\left(i_{q\text{ref}} - i_q\right)dt \tag{9}$$

$$R_s I_{sd} + L_s \frac{dI_{sd}}{dt} = k_{p1}(i_{d\text{ref}} - i_d) + k_{i1}\int(i_{d\text{ref}} - i_d)dt \tag{10}$$

where R_s is the generator resistance, L_s is the generator inductance, and Ω is the rotor rotational speed. Owing to the aligned stator flux with the reference frame, then the *q*-axis of the stator flux is set to zero $(\varphi_{sq} = 0)$ and consequently $(\varphi_s = \varphi_{sd})$. From (9) and (10), k_{p1} and k_{i1} represent PI controllers' gains of the inner current controllers.

3.3.2 Control strategy for grid side VSC connected to wind farm AC bus: In the case of the installed VSC at the AC bus side, the DC bus voltage can be regulated by the *d*-axis current component and maintained constant following its reference value. Furthermore, the *q*-axis current component is controlling *Q* and is kept zero to deliver no reactive power in the grid. The line voltage across VSC can be introduced as follows:

$$V_q = V_{\text{pcc},q} + L\,\omega\,i_d + \left(R\,i_q + L\frac{di_q}{dt}\right) \tag{11}$$

$$V_d = V_{\text{pcc},d} - L\,\omega\,i_q + \left(R\,i_d + L\frac{di_d}{dt}\right) \tag{12}$$

with

$$\left(Ri_d + L\frac{di_d}{dt}\right) = k_{p2}(i_{d\text{ref}} - i_d) + k_{i2}\int(i_{d\text{ref}} - i_d)dt \tag{13}$$

$$\left(Ri_q + L\frac{di_q}{dt}\right) = k_{p2}\left(i_{q\text{ref}} - i_q\right) + k_{i2}\int\left(i_{q\text{ref}} - i_q\right)dt \tag{14}$$

where $V_{\text{pcc},d}$ and $V_{\text{pcc},q}$ are the voltage terminal across resistor–inductor (RL) filter, *R* and *L* are the series filter resistance and reactance to filter the high-frequency ripple owing to the converter devices switching, and ω is the angular frequency of the voltage terminal across the RL filter

From (13) and (14), k_{p2} and k_{i2} are PI parameters' gains of the inner current controllers, taking into consideration that the signal $i_{d\text{ref}}$ is the reference active component, which is derived from the outer DC voltage circuit as in (15)

$$i_{d\text{ref}} = k_{p3}(V_{\text{dc,ref}} - V_{\text{dc}}) + k_{i3}\int(V_{\text{dc,ref}} - V_{\text{dc}})dt \tag{15}$$

where k_{p3} and k_{i3} are PI controllers' gains of the DC voltage circuit controller.

4 VSC-based HVDC transmission system

4.1 System configuration

VSC–HVDC composed of a pair of three-level neutral point clamped (NPC) with selectable topologies and power switching devices at onshore and offshore HVDC stations. In the high-voltage (HV) application, multilevel VSC configuration is more appropriate especially in harmonic performance and withstanding high currents.

Three-level VSC (or called NPC–VSC) is considered one of the main VSC configurations that are utilised in the DC transmission system. In a huge power plant application, the topology of NPC–VSC is more efficient to use, which consists of four bridges for every branch [25]. In NPC–VSC system configuration, extra six diodes are constructed in the centre of the DC link, and switches are used to boost the abilities of the VSC' voltage blocking and accordingly increment the HVDC ratings. In this study, the length of the HV underground cable is assumed as 75 km. Table 2 presents the cable [5] and converter parameters [39].

The OWF is connected to the VSC–HVDC station through an AC filter to prohibit any harmonics induced in the output voltage of the PMSG owing to insulated gate bipolar transistor switching, and a phase reactor to control P and Q flow by means of the current regulation.

4.2 System modelling and control strategy

The power converter and inverter utilised in the offshore and onshore VSC stations, respectively, are illustrated in Fig. 1. The main configurations and strategies of the control techniques used in the two stations are clearly descripted in the following clauses in detail [40–42].

4.2.1 Offshore VSC station connected with wind farm: The offshore VSC station is directly connected to the HVDC transmission line at the sending end as indicated in Fig. 1, where VSC with vector control technique consists of four control circuits, two circuits for inner current controllers to regulate the currents i_{sd} and i_{sq} and another two circuits for outer voltage controllers to regulate V_{dc} at the transmission system sending end at constant level; and to maintain root-mean square (r.m.s.) voltage at PCC1 (i.e. indicated in Fig. 1) at constant level. The reference values of the inner current controllers have been generated by the outer controller and then processed to the inner current controller circuit.

The mathematical model of the inner current loop of the cascaded controller related to offshore VSC station in the *dq* synchronous reference frame is expressed in the following equations:

$$V_{c,d} = V_{\text{pcc},d} + \omega L i_q - \left(Ri_d + L\frac{di_d}{dt}\right) \tag{16}$$

$$V_{c,q} = V_{\text{pcc},q} - \omega L i_d - \left(Ri_q + L\frac{di_q}{dt}\right) \tag{17}$$

with

$$\left(Ri_d + L\frac{di_d}{dt}\right) = k_{p6}(i_{d\text{ref}} - i_d) + k_{i6}\int(i_{d\text{ref}} - i_d)dt \tag{18}$$

$$\left(Ri_q + L\frac{di_q}{dt}\right) = k_{p6}\left(i_{q\text{ref}} - i_q\right) + k_{i6}\int\left(i_{q\text{ref}} - i_q\right)dt \tag{19}$$

where i_d and i_q are the dq-axis values of PCC1 bus currents, $V_{c,d}$ and $V_{c,q}$ are dq-axis values of VSC AC voltages, R is the transformer's resistance, L is the inductance of the transformer and phase reactor, ω is the system angular frequency, $\omega L i_d$ and $\omega L i_q$ components present the decoupling compensation; $V_{pcc,d}$ and $V_{pcc,q}$ are the dq-axis values of PCC1 bus voltages.

From (18) and (19), k_{p6} and k_{i6} are PI parameters' gains of the inner current controllers, taking into consideration that the signals $i_{d\text{ref}}$ and $i_{q\text{ref}}$ are the reference active and reactive components that resulted from the outer voltage circuit as follows:

$$i_{d\text{ref}} = k_{p4}(V_{\text{dc,ref}} - V_{\text{dc}}) + k_{i4}\int (V_{\text{dc,ref}} - V_{\text{dc}})\text{d}t \tag{20}$$

$$i_{q\text{ref}} = k_{p5}(V_{\text{pcc,ref}} - V_{\text{pcc}}) + k_{i5}\int (V_{\text{pcc,ref}} - V_{\text{pcc}})\text{d}t \tag{21}$$

where k_{p4} and k_{i4} are PI parameters' gains of the DC link voltage controller, however, k_{p5} and k_{i5} are PI parameters' gains of AC voltage controller.

4.2.2 Onshore VSC station connected with global AC grid: The topology of the onshore VSC station at the receiving end is the same as in the offshore VSC station at the sending end, and the mathematical model of the onshore converter installed at the AC grid side is similar to the mentioned before but with the following coefficient gains:

- k_{p7} and k_{i7} are PI parameters' gains of the DC link voltage controller.
- k_{p8} and k_{i8} are PI parameters' gains of the AC voltage controller.
- k_{p9} and k_{i9} are PI parameters' gains of the inner current controllers.

5 Optimisation design of cascade PI controller

An optimisation algorithm is a powerful tool, which is used to design the controllers' parameters. Optimisation issues are becoming one of the leading research domains. In the recent decade, a lot of research studies had drawn attention to meta-heuristic algorithms owing to the traditional techniques, however, it shall be noted that these algorithms are not sufficient for fixing the complicated optimisation problems.

Meta-heuristic techniques are particularly inspired by the behaviour of animals and their evolutionary theories. Meta-heuristic techniques are powerful, robust, flexible, and simple characterised.

In this work, owing to the system model non-linearity, the sum of integral square errors (ISE) of V_{dc} across the capacitor at wind system is used as a first fitness function as represented in the cost function (22), while the sum of ISE of V_{dc} at the transmission (sending or receiving) end and r.m.s. voltage at PCC (1 or 2) are used as a second fitness function as represented in cost function (23)

$$\text{Fitness} = \sum \text{ISE} = \int (V_{\text{dc,ref}} - V_{\text{dc}})^2 \text{d}t \tag{22}$$

$$\text{Fitness} = \sum \text{ISE} = \int (V_{\text{dc,ref}} - V_{\text{dc}})^2 \text{d}t + \int (V_{\text{pcc,ref}} - V_{\text{pcc}})^2 \text{d}t \tag{23}$$

5.1 GWO algorithm overview

GWO algorithm is deemed one of the recent algorithms in meta-heuristic optimisation techniques and it is highly effective to transact with the optimisation problems.

GWO algorithm simulates the pack lifestyle of the grey wolves actually in nature concerning hierarch of society and hunting techniques [31–34]. The selected types of grey wolves are α, β, δ, and ω. They are specified to simulate the structure of hierarchy. The fundamental steps of the hunting process for optimisation execution are searching/tracking the prey then encircling/harassing the prey, and eventually attack the prey. The great merits of the GWO algorithm are more simple, flexible, and lacking derivatives.

The creation of a random population of grey wolves is the first step of the GWO optimisation procedure. Along with the iterations, the possible position of the prey can be estimated by α, β, and δ wolves to represent the optimal solution. According to the distances of the grey wolves from the prey, they update their positions.

5.2 CSA overview

CSA is one of the meta-heuristic algorithms, which is inspired by nature. CSA is a population-based stochastic optimisation algorithm and it has great search abilities. CSA has memory mechanisation for helping to record the local minimal and participate to pick out the best [43–47]. As a result, CSA can look for the best optimum value through the specified search space in a better approach than other techniques. CSA is inspiring from a sort of bird called cuckoo bird owing to its various lifestyles and encroach reproductivity [43–47].

The basic steps of CSA are as follows:

- The cuckoo lays one egg every time.
- The cuckoo throws down its egg in a random nest.
- The best nests of high-quality eggs only will be transferred to the following generation. The obtainable host nests number is constant.

5.3 Hybrid CSA–GWO overviews

Recently, hybridisation of two or more algorithms is recently trended to detect the superior solutions of the optimisation troubles. Many collections of familiar optimisation techniques have been incorporated in hybrid optimised algorithms to become more efficient to deal with the practical issues.

GWO inspects an individual with a high fitness value, and accordingly a weak ability of global search occurs and subject to fall-into the local optimum easier. CSA updates the nest's positions with a certain probability independent of the search path, and with random directions. So, in CSA, it is much easier to jump from the current region to another. Based on this, CSA is a very helpful tool for GWO improvement. This means CSA is used to update the positions of current search agents and obtain a new set. The flowchart of GWO integrated with CSA is as represented in Fig. 2.

As previously described, one of the most recent combinations of optimisation techniques is the GWO algorithm with the CSA, where the key group parameters in GWO are updated by cuckoo search's position updating formula as clearly described in the flow chart. The new hybrid CSA–GWO is powerful and capable of finding an efficient solution to optimisation problems.

In this concern, the position updated equation of CSA is applied to amend the positions, convergence accuracies, and speeds of the grey wolf agent (α) for purpose of balancing among exploring, exploiting, and expanding convergence behaviours of the GWO algorithm, while the remaining process of the GWO algorithm considered as it is. The analytical and statistical solutions obtained using the new hybrid approach CSA–GWO is compared with another meta-heuristics approach such as GA to examine the efficiencies of the design parameters.

6 Simulation analysis and verification

A cost function name is commonly used to represent the objective function, where it obtains the variables in a vector and then retunes the objective value. In this study, the intended design variables are PI parameters' gains included in all highlighted VSC stations as illustrated in the above equations provided that the range of these design variables is from 0 to 100.

The efficiency and efficacy of the offered algorithm have been investigated by simulations through the following transient and dynamic studied scenarios. The mentioned parameters in Table 1 were applied to the built-in model of the PMSG wind turbine included in the MATLAB/Simulink libraries.

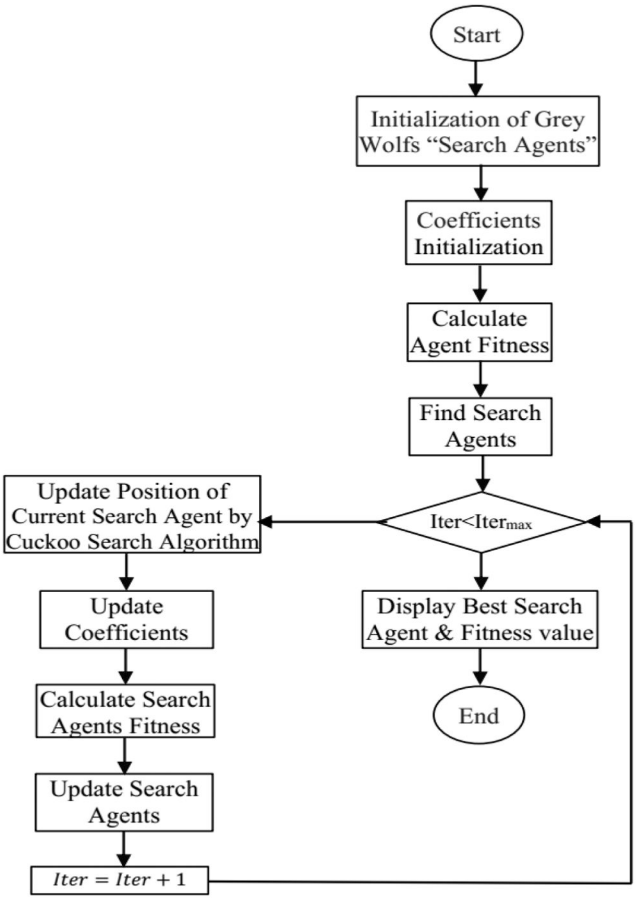

Fig. 2 *Flowchart of optimal design procedure using hybrid CSA–GWO Algorithm*

Table 3 Optimal setting for the new hybrid CSA–GWO

Parameter	Setting
no. of iterations	100
no. of search agents	10
lower boundary limit	0
upper boundary limit	100
no of variables	4

Table 4 Optimal setting for GA [25]

Parameter	Setting
no. of iterations	100
lower boundary limit	0
upper boundary limit	100
no of variables	4

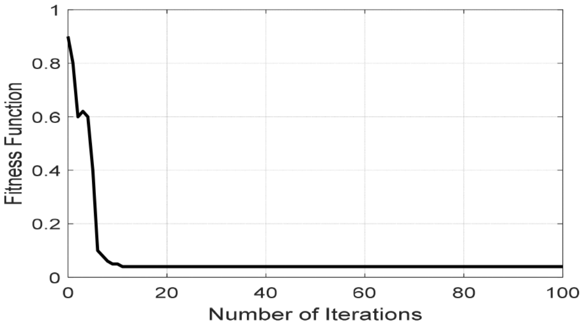

Fig. 3 *Fitness function convergence using the new hybrid*

6.1 Transient characteristics analysis

FRT requirements are enjoined on the wind generation system to keep system stabilisation and connection with the network even during a fault, where the wind farm disconnecting from the main grid is representing a worst and critical situation for this grid. In this regard, the following symmetrical and unsymmetrical faulted cases are deemed to check the efficiency and validity of the control strategy using the optimal values of VSC by using the new hybrid CSA–GWO as clarified in Section 5. Table 3 represents the optimal settings for the new hybrid algorithm controller, while Table 4 is for GA. The fitness function convergence is as illustrated in Fig. 3.

To examine the effectiveness of the offered hybrid algorithm-based optimisation technique, a comparison with the GA method can be exhibited.

It shall be noted that GA is one of the efficient optimised methods utilised in power systems. Both optimised techniques are implemented using the optimisation toolbox of MATLAB software [39]. Tables 5 and 6 show the optimal values for all gains used in the studied configuration model.

The outcomes of simulation can be clarified in the following cases.

Table 5 Optimal design for PI controller parameters by the new hybrid algorithm

Location	PI parameters	CSA–GWO k_p	CSA–GWO k_i
wind system	k_{p1} and k_{i1}	3.9103	37.4568
	k_{p2} and k_{i2}	0.9648	2.7775
	k_{p3} and k_{i3}	19.8615	83.8504
offshore station	k_{p4} and k_{i4}	14.0518	34.5888
	k_{p5} and k_{i5}	7.6275	25.5542
	k_{p6} and k_{i6}	0.6870	71.1768
onshore station	k_{p7} and k_{i7}	11.1360	82.9617
	k_{p8} and k_{i8}	5.7257	9.9409
	k_{p9} and k_{i9}	1.2073	19.3399

Table 6 Optimal design for PI controller parameters by GA

Location	PI parameters	GA k_p	GA k_i
wind system	k_{p1} and k_{i1}	15.6187	5.6171
	k_{p2} and k_{i2}	0.858	1.959
	k_{p3} and k_{i3}	74.31	82.846
offshore station	k_{p4} and k_{i4}	0.589	87.937
	k_{p5} and k_{i5}	13.835	18.179
	k_{p6} and k_{i6}	1.587	9.689
onshore station	k_{p7} and k_{i7}	37.828	61.81
	k_{p8} and k_{i8}	8.955	7.995
	k_{p9} and k_{i9}	1.6	10

6.1.1 Case 1, symmetrical three-phase to ground fault: For the transient stability analysis using symmetrical fault simulation as a network disturbance (fault occurred at instant 4.1 s and Circuit Breaker (CB) of faulty line is opened at 4.22 s, and then reclose again at 5.5 s), three-phase to ground fault at the grid side (at point F as indicated in Fig. 1) is considered using the new hybrid CSA–GWO and GA methods.

Fig. 4*a* presents the DC-voltage waveform of DC-link at wind farm configuration. Fig. 4*b* presents the DC-voltage waveform at the transmission network, whilst Figs. 4*c* and *d* show r.m.s. voltages waveforms at PCC1 and PCC2, respectively. Noting that all waveforms are represented using the new approach hybrid CSA–GWO and compared with the GA technique. The indicated ripples resulted in owing to the high frequency of the switching of the power electronic devices.

As presented in Fig. 4, maximum percent overshoot (MPOS), minimum present undershoot (MPUS), settling time (Ts) and steady-state error (Ess) of the r.m.s. and DC voltages profiles using the new hybrid CSA–GWO algorithm is much better comparing with those using GA in case of the symmetrical 3LG fault occurrence at the grid.

From Fig. 4, it can be realised that all voltage waveforms can return back to their pre-fault levels, and it is clearly demonstrated that when using the new hybrid CSA–GWO, a good damping response can be obtained compared with GA.

6.1.2 Case 2, unsymmetrical phase to ground fault: For more verification concerning the offered algorithm, the transient stability analysis using unsymmetrical fault simulation is carried out as a network disturbance considering line-to-ground (LG) fault at the same location using the new hybrid CSA–GWO and GA algorithms.

In this case, MPOS, MPUS, Ts and Ess of the DC voltages of the transmission line and the r.m.s. voltages at PCC1 and PCC2 response using the new hybrid CSA–GWO have been better damping than that resulted from GA algorithm, as illustrated in Fig. 5.

6.1.3 Case 3, unsymmetrical line to line (LL) fault: The transient stability analysis using unsymmetrical fault simulation is carried out as a network disturbance considering LL fault at the same location using the new hybrid CSA–GWO algorithm and GA. Repeated the above but with an unsymmetrical LL fault with the same conclusions, as shown in Fig. 6.

In this case, MPOS, MPUS, Ts, and Ess of the DC voltages of the transmission line and r.m.s. voltages at PCC1 and PCC2 response using the new hybrid CSA–GWO have been better damping than that resulted from GA, as illustrated in Fig. 6.

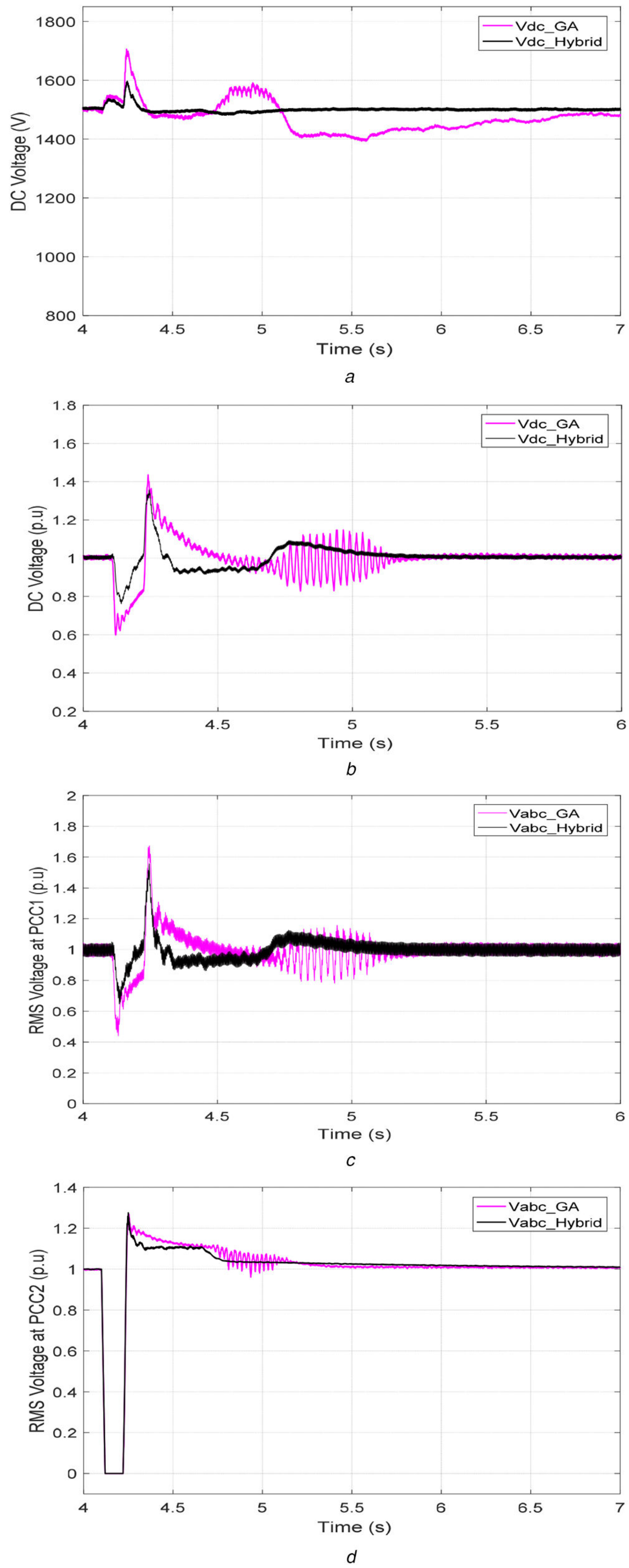

Fig. 4 *Transient response for 3LG fault occurs*
(a) DC voltage across capacitors of VSC at wind farm system, ***(b)*** DC voltage at the transmission network, ***(c)*** r.m.s. voltage at PCC1, ***(d)*** r.m.s. voltage at PCC2

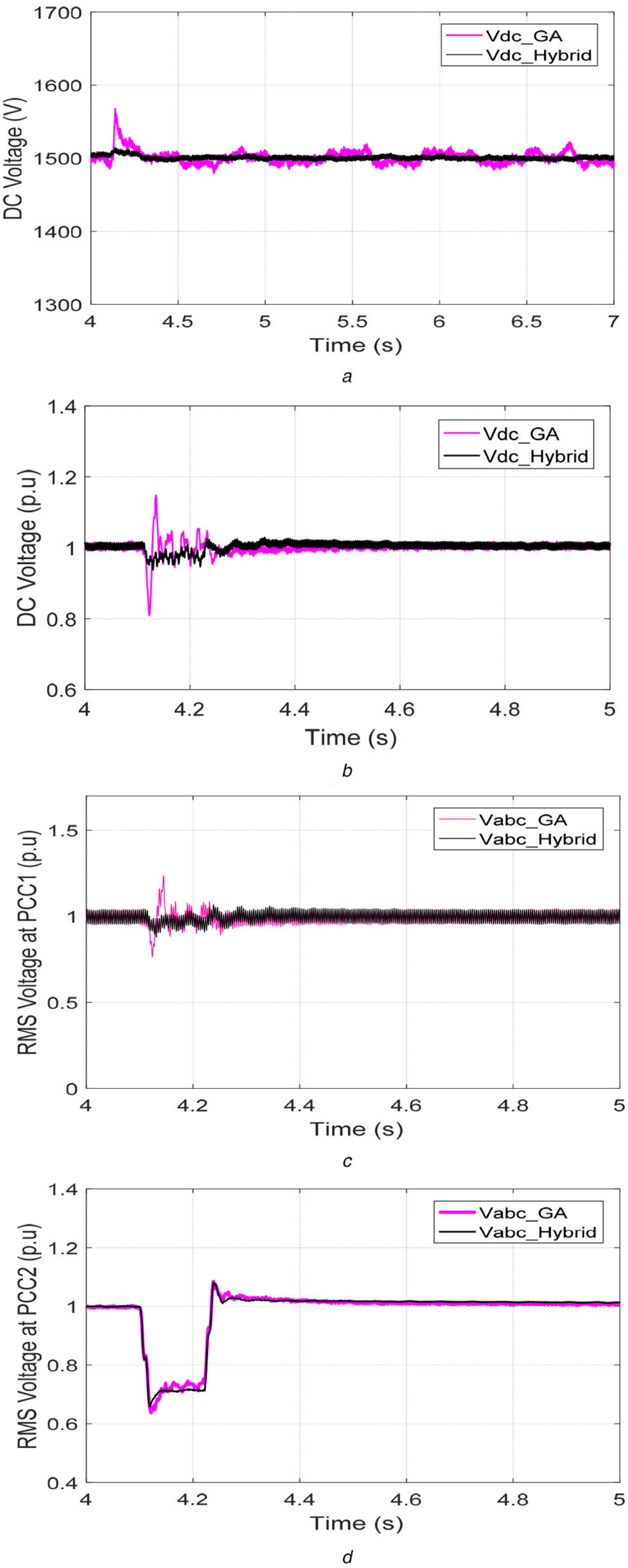

Fig. 5 *Transient response for LG fault occurs*
(a) DC voltage across capacitors of VSC at wind farm system, ***(b)*** DC voltage at the transmission network, ***(c)*** r.m.s. voltage at PCC1, ***(d)*** r.m.s. voltage at PCC2

6.1.4 Case 4, unsymmetrical double phase to ground fault: For more verification concerning the offered algorithm, the transient stability analysis using unsymmetrical fault simulation is carried out as a network disturbance considering 2LG fault at the same location using the new hybrid CSA–GWO algorithm and GA.

In this case, MPOS, MPUS, Ts, and Ess of the DC voltages of the transmission line and the r.m.s. voltages at PCC1 and PCC2 response using the new hybrid CSA–GWO have been better damping than that resulted from GA, as illustrated in Fig. 7.

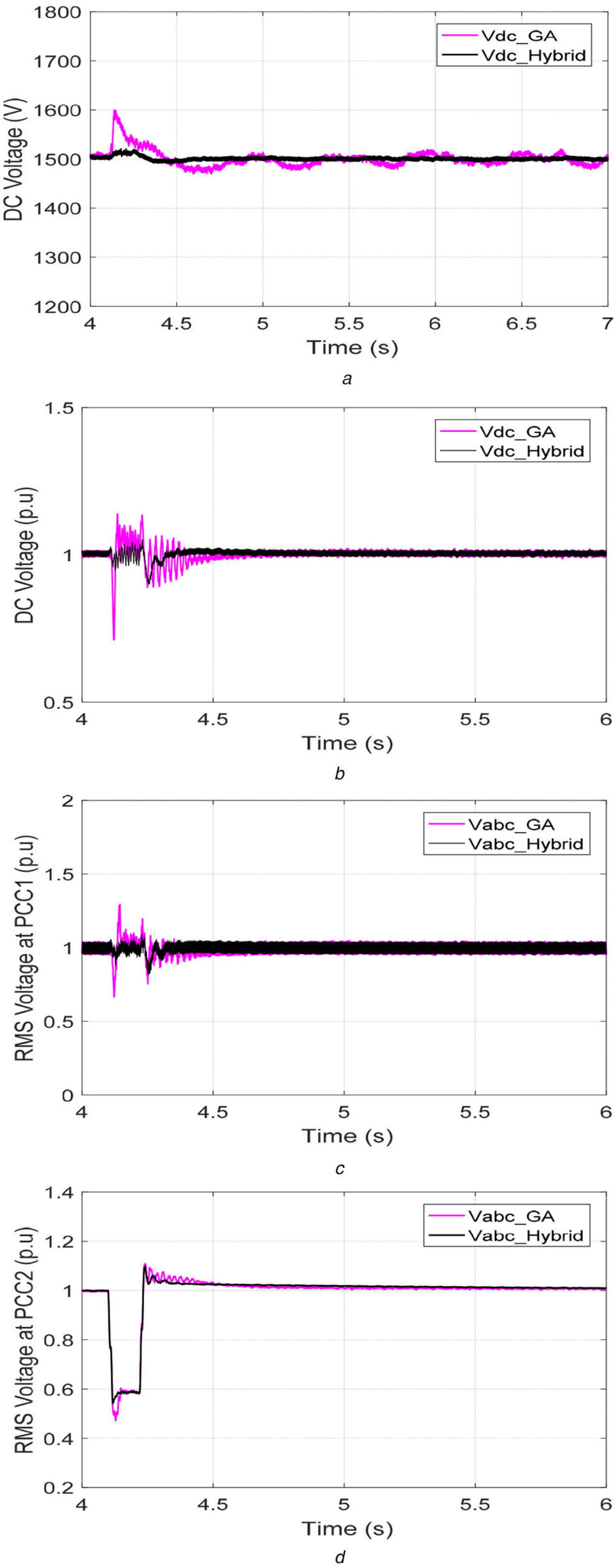

Fig. 6 *Transient response for LL fault occurs*
(a) DC voltage across capacitors of VSC at the wind farm system, ***(b)*** DC voltage at the transmission network, ***(c)*** r.m.s. voltage at PCC1, ***(d)*** r.m.s. voltage at PCC2

In reference to the simulated results of the studied scenarios and as a conclusion for the different faulty conditions, the FRT of OWF-based HVDC is improved when the new hybrid CSA–GWO algorithm is used to provide the PI controllers' parameters.

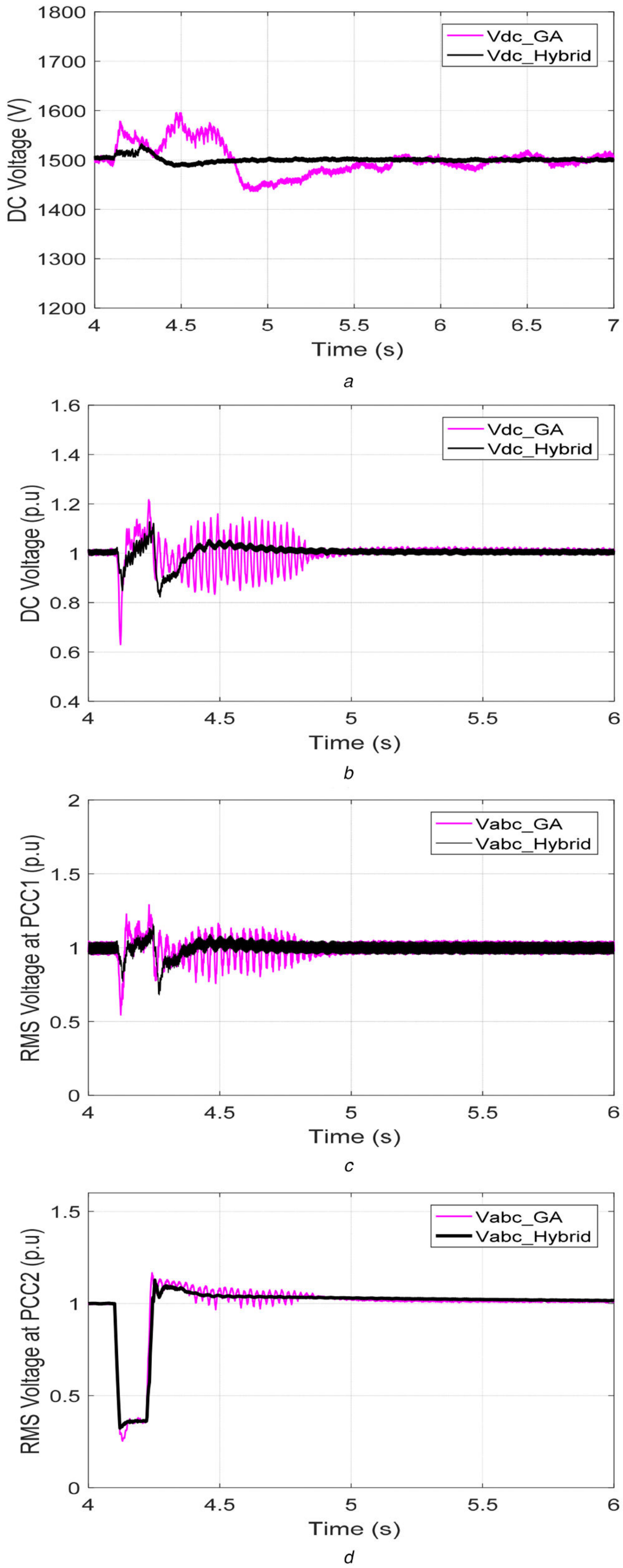

Fig. 7 *Transient response for 2LG fault occurs*
(a) DC voltage across capacitors of VSC at the wind farm system, ***(b)*** DC voltage at the transmission network, ***(c)*** r.m.s. voltage at PCC1, ***(d)*** r.m.s. voltage at PCC2

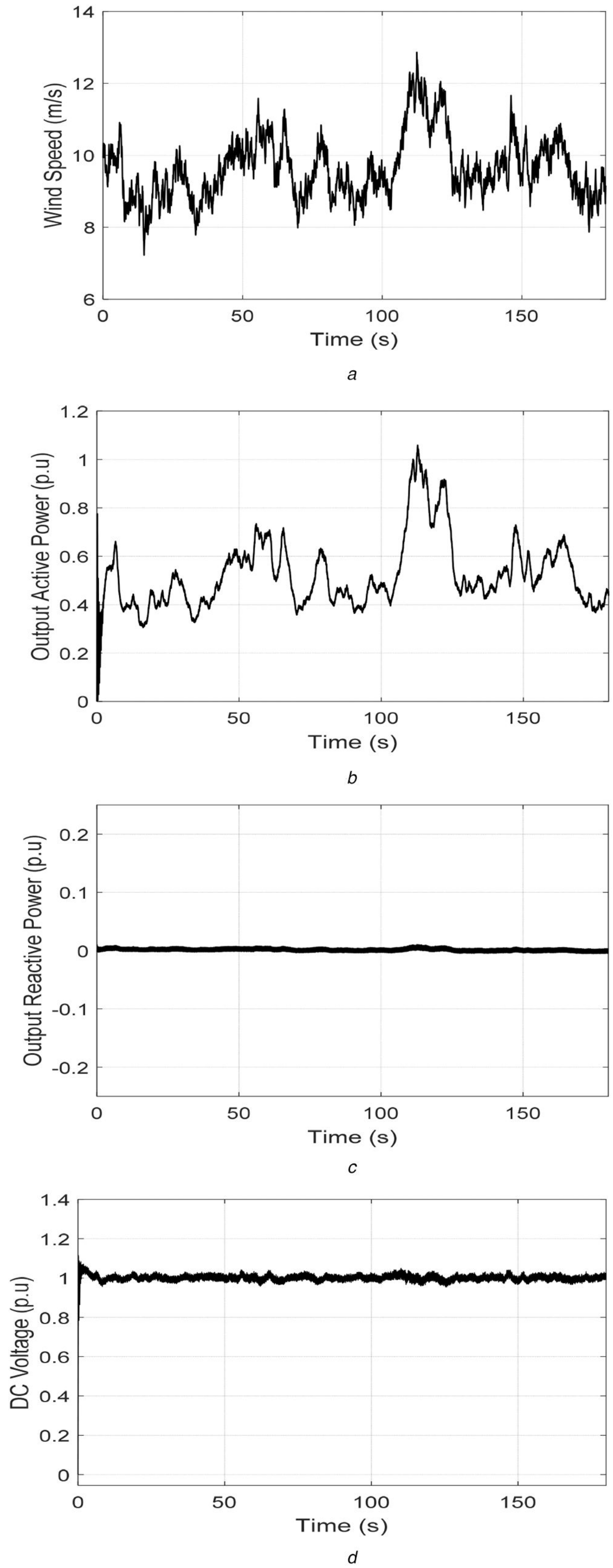

Fig. 8 *Dynamic characteristics of the OWF*
(a) Actual wind speed, ***(b)*** Measured output active power, ***(c)*** Measured output reactive power, ***(d)*** DC voltage across capacitors of VSC

6.2 Dynamic characteristics analysis

To examine the controllers' response during the wind speed fluctuation, VSWT–PMSG dynamic characteristics are checked using an actual wind speed log recorded at the Zafarrana wind site in Egypt [4]. Fig. 8*a* presents the wind speed variations for the 180 s period, which was simulated and implemented using MATLAB/Simulink software with the new hybrid CSA–GWO algorithm. As cleared, 180 s pattern of the wind speed fluctuates between 7.3 and 12.7 m/s.

Concerning the machine side converter with a direct connection to the PMSG, the responses of actual measured active and reactive powers versus the reference values at different wind speeds for the wind turbine generator system are presented in Figs. 8*b* and *c*, considering that Q_{ref} is zero to obtain an operation with a unity power factor. Also, the maintained DC bus voltage of the wind farm system that resulted from using the grid side converter is illustrated in Fig. 8*d*.

From the dynamic characteristics' analysis, the new hybrid CSA–GWO is deemed as an efficient algorithm used to extract the maximum possible power from the wind source under any different operational conditions.

7 Conclusions

In this study, an optimal design process to determine the multiple PI controllers' parameters utilised in the cascaded control principle is presented for VSC-based VSWT–PMSG and VSC-based HVDC (at offshore and onshore stations) using the new hybrid CSA–GWO. The offered algorithm is used in the VSC system to avoid any complexity or complication to define the overall system transfer function.

The effectiveness of the optimisation process using two designing algorithms has been proven throughout this study. The results evinced that the new hybrid CSA–GWO had more desirable optimum solutions than others. It gives excellent performance with dynamic analysis as well as the transient analysis. This dynamic performance is evaluated using a real wind speed pattern. It is observed that the new hybrid CSA–GWO has a better damped performance comparing with GA specially to fulfil the FRT capabilities of OWF connected with the electrical grid through the HVDC transmission system. Finally, it is concluded that the new hybrid CSA–GWO algorithm is considered an excellent choice for the optimal design of the PI parameters' gains for VSC-based VSWT–PMSG and VSC-based HVDC.

8 References

[1] Hasanien, H.M., Muyeen, S.M.: 'A Taguchi approach for optimum design of proportional–integral controllers in cascaded control scheme', *IEEE Trans. Power Syst.*, 2013, **28**, pp. 1636–1644

[2] Ahuja, H., Singh, A., Sharma, A.: 'Large scale wind energy conversion system using permanent magnet synchronous generator'. 2014 Innovative Applications of Computational Intelligence on Power, Energy, and Controls with their impact on Humanity (CIPECH), Ghaziabad, India, 2014, pp. 279–284

[3] Mahmoud, H.Y., Besheer, A.H., Hasanien, H.M., *et al.*: 'Different control strategies for converter based DC energy transmission in offshore wind power: a literature survey'. 2018 Twentieth Int. Middle East Power Systems Conf. (MEPCON), Cairo, Egypt, 2018, pp. 190–197

[4] Soliman, M.A., Hasanien, H.M., Azazi, H.Z., *et al.*: 'An adaptive fuzzy logic control strategy for performance enhancement of a grid connected PMSG based wind turbine', *IEEE Trans. Ind. Inf.*, 2019, **15**, pp. 3163–3173

[5] Muyeen, S.M., Takahashi, R., Tamura, J.: 'Operation and control of HVDC connected offshore wind farm', *IEEE Trans Sustain Energy*, 2010, **1**, pp. 30–37

[6] Benadja, M., Chandra, A.: 'Adaptive sensorless control of PMSGs-based offshore wind farm and VSC-HVDC stations', *IEEE J. Emerg. Sel. Top. Power Electron.*, 2015, **3**, pp. 918–931

[7] Hasanien, H.M., Muyeen, S.M.: 'Operation and control of HVDC stations using continuous mixed p-norm based adaptive fuzzy technique', *IET Gener. Transm. Distrib.*, 2017, **11**, pp. 2275–2282

[8] Hasanien, H.M., Muyeen, S.M.: 'Affine projection algorithm based adaptive control scheme for operation of variable-speed wind generator', *IET Gener. Transm. Distrib.*, 2015, **9**, pp. 2611–2616

[9] Qais, M.H., Hasanien, H.M., Alghuwainem, S.: 'Whale optimization algorithm-based Sugeno fuzzy logic controller for fault ride-through improvement of grid-connected variable speed wind generators', *Eng. Appl. Artif. Intell.*, 2020, **87**, pp. 1–13

[10] Khani, N.G., Abedi, M., Gharehpetian, G.B., *et al.*: 'Offshore wind farm power control using HVDC link', *Can. J. Electr. Comput. Eng.*, 2016, **39**, pp. 168–173

[11] Soliman, M.A., Hasanien, H.M., Azazi, H.Z., *et al.*: 'Linear-quadratic regulator algorithm-based cascaded control scheme for performance enhancement of a variable-speed wind energy conversion system', *Arab. J. Sci. Eng.*, 2019, **44**, (3), pp. 2281–2293

[12] Camara, M.S., Camara, M.B., Dakyo, B., *et al.*: 'Permanent magnet synchronous generators for offshore wind energy system linked to grid-modeling and control strategies'. 16th Int. Power Electronics & Motion Control Conf. & Exposition, Antalya, Turkey, 2014, pp. 114–118

[13] Muyeen, S.M., Al-Durra, A.: 'Modeling and control strategies of fuzzy logic controlled inverter system for grid interconnected variable speed wind generator', *IEEE Syst. J.*, 2013, **7**, pp. 817–824

[14] Li, Y., Ang, K.H., Chong, G.C.Y.: 'PID control system analysis and design, problems, remedies, and future directions', *IEEE Control Syst. Mag.*, 2006, **26**, (1), pp. 32–41

[15] Mazouz, L., Zidi, S.A., Khatir, M., *et al.*: 'Particle swarm optimization based PI controller of VSC-HVDC system connected to a wind farm'. The Society for Reliability Engineering, Quality and Operations Management (SREQOM), India, 2015

[16] Huang, D., Mao, Y.: 'The study of control strategy for VSC-HVDC applied in offshore wind farm and grid connection'. Asia-Pacific Power and Energy Engineering Conf., Wuhan, People's Republic of China, 2011, pp. 1–4

[17] Soliman, M.A., Hasanien, H.M., Alghuwainem, S., *et al.*: 'Symbiotic organisms search algorithm-based optimal control strategy for efficient operation of variable-speed wind generators', *IET Renew. Power Gener.*, 2019, **13**, pp. 2684–2692

[18] Hasanien, H.M., El-Fergany, A.A.: 'Symbiotic organisms search algorithm for automatic generation control of interconnected power systems including wind farms', *IET Gener. Transm. Distrib.*, 2017, **11**, pp. 1692–1700

[19] Qi, S.R., Wang, D.F., Han, P., *et al.*: 'Grey prediction based RBF neural network self-tuning PID control for turning process'. Proc. Int. Conf. on Machine Learning and Cybernetics, Shanghai, China, 2004, pp. 802–805

[20] Rubaai, A., Castro-Sitiriche, M.J., Ofoli, A.R.: 'Design and implementation of parallel fuzzy PID controller for high-performance brushless motor drives: an integrated environment for rapid control prototyping', *IEEE Trans. Ind. Appl.*, 2008, **44**, (4), pp. 1090–1098

[21] Besheer, A.H.: 'Tuning method for PID control scheme: A blended ant system optimization technique with Takagi Sugeno fuzzy system'. ICFC Int. Conf. on Fuzzy Computation, Valencia, Spain, 2010, pp. 113–119

[22] Taj, T.A., Hasanien, H.M., Alolah, A.I.: 'Transient stability enhancement of a grid-connected wind farm using an adaptive neuro-fuzzy controlled-flywheel energy storage system', *IET Renew. Power Gener.*, 2015, **9**, pp. 792–800

[23] Rubaai, A., Young, P.: 'EKF-based PI-/PD-like fuzzy-neural-network-controller for brushless drives', *IEEE Trans. Ind. Appl.*, 2011, **47**, (6), pp. 2391–2401

[24] Soliman, M.A., Hasanien, H.M., Azazi, H.Z., *et al.*: 'Hybrid ANFIS-GA-based control scheme for performance enhancement of a grid-connected wind generator', *IET Renew. Power Gener.*, 2018, **12**, (7), pp. 832–843

[25] Hasanien, H.M., Muyeen, S.M.: 'Design optimization of controller parameters used in Variable speed wind energy conversion system by genetic algorithms', *IEEE Trans. Sustain Energy*, 2012, **3**, pp. 200–208

[26] Devaraj, D., Selvabala, B.: 'Real-coded genetic algorithm and fuzzy logic approach for real-time tuning of proportional–integral–derivative controller in automatic voltage regulator system', *IET Gener. Transm. Distrib.*, 2009, **3**, (7), pp. 641–649

[27] Zhang, J., Zhuang, J., Du, H., *et al.*: 'Self-organizing genetic algorithm based tuning of PID controllers', *Inf. Sci.*, 2009, **179**, (7), pp. 1007–1018

[28] Hasanien, H.M., Muyeen, S.M.: 'Particle swarm optimization based superconducting magnetic energy storage for low-voltage ride through capability enhancement in wind energy conversion system', *Electr. Power Compon. Syst.*, 2015, **43**, (11), pp. 1278–1288

[29] Mukherjee, V., Ghoshal, S.P.: 'Intelligent particle swarm optimized fuzzy PID controller for AVR system', *Electr. Power Syst. Res.*, 2007, **77**, pp. 1689–1698

[30] Gaing, Z.-L.: 'A particle swarm optimization approach for optimum design of PID controller in AVR system', *IEEE Trans. Energy Convers.*, 2004, **19**, (2), pp. 384–391

[31] Qais, M.H., Hasanien, H.M., Alghuwainem, S.: 'A grey wolf optimizer for Optimum parameters of multiple PI controllers of a grid-connected PMSG driven by variable speed wind turbine', *IEEE Access*, 2018, **6**, pp. 44120–44128

[32] El-Fergany, A.A., Hasanien, H.M.: 'Single and multi-objective optimal power flow using grey wolf optimizer and differential evolution algorithms', *Electr. Power Compon. Syst.*, 2015, **43**, pp. 1548–1559

[33] Sharma, S., Salgotra, R., Singh, U.: 'An enhanced grey wolf optimizer for numerical optimization'. Int. Conf. on Innovations in Information, Embedded and Communication Systems (ICIIECS), Coimbatore, India, 2017, pp. 1–6

[34] Mirjalili, S., Mirjalili, S.M., Lewis, A, *et al.*: 'Grey wolf optimizer', *Adv. Eng. Softw.*, 2014, **69**, pp. 46–61

[35] Årdal, A.R., D'Arco, S., Torres-Olguin, R.E., *et al.*: 'Parametric sensitivity of transients in an islanded system with an offshore wind farm connected to an oil platform'. Proc. 14th European Conf. on Power Electronics and Applications, Birmingham, UK, 2011, pp. 1–10

[36] Heydari, M., Smedley, K.: 'Comparison of maximum power point tracking methods for medium to high power wind energy system'. 2015 20th Conf. on Electrical Power Distribution Networks Conf. (EPDC), Zahedan, Iran, 2015, pp. 184–189

[37] Shukla, P., Tiwari, N., Shimi, S.L.: 'Maximum power point tracking control for wind energy conversion system: a review', *Int. J. Adv. Res. Electr., Electron. Instrum. Eng.*, 2015, **4**, pp. 5239–5244

[38] Errami, Y., Ouassaid, M., Maaroufi, M.: 'Control of a PMSG based wind energy generation system for power maximization and grid fault conditions'. Mediterranean Green Energy Forum MGEF-13, Fes, Morocco, 2013, pp. 220–229

[39] Release R2016a.: '*MATLAB optimization toolbox*' (The Math Works Press, Cambridge, UK, 2016)

[40] Xiaoguang, W., Guangfu, T.: 'Research of AC/DC parallel wind farm integration based on VSC–HVDC'. 2006 Int. Conf. on Power System Technology, Chongqing, People's Republic of China, 2006, pp. 1–5

[41] Giddani, O.A., Adam, G.P., Anaya-Lara, O., *et al.*: 'Control strategies of VSC–HVDC transmission system for wind power integration to meet GB grid code requirements, International Symposium on Power Electronics, Electrical Drives, Automation and Motion (SPEEDAM), Pisa, Italy, 2010, pp. 385–390

[42] Xinnan, Z., Jiayi, L. Yangshuo: 'The control method and experimental study of HVDC light inverter part'. IEEE Power Engineering and Automation Conf., Wuhan, People's Republic of China, 2011, pp. 268–271

[43] Mareli, M., Twala, B.: 'An adaptive cuckoo search algorithm for optimisation', *Appl. Comput. Inf.*, 2018, **14**, (2), pp. 107–115

[44] Hasanien, H.M., Hashem, G.M.: ‘A cuckoo search algorithm optimizer for steady-state analysis of self-excited induction generator’, *Ain Shams Eng. J.*, 2018, **9**, pp. 2549–2555
[45] Joshi, A.S., Kulkarni, O., Kakandikar, G.M.*, et al.*: ‘Cuckoo search optimization – a review’. Int. Conf. on Advancements in Aeromechanical Materials for Manufacturing (ICAAMM-2016), Hyderabad, India, 2017, pp. 7262–7269
[46] Kalaam, R.N., Muyeen, S.M., Al-Durra, A.*, et al.*: ‘Optimisation of controller parameters for grid tied photovoltaic system at faulty network using artificial neural network-based cuckoo search algorithm’, *IET Renew. Power Gener.*, 2017, **11**, (12), pp. 1517–1526
[47] Peram, M., Mishra, S., Vemulapaty, M.*, et al.*: ‘Optimal PI–PD and I–PD controller design using cuckoo search algorithm’. 2018 5th Int. Conf. on Signal Processing and Integrated Networks (SPIN), Noida, India, 2018, pp. 643–646